Drag reduction in turbulent channel flow using bidirectional wavy Lorentz force

HUANG LePing[1,2], CHOI KwingSo[3*], FAN BaoChun[2] & CHEN YaoHui[2]

[1] *Xi'an Aerospace Propulsion Institute, Xi'an 710100, China;*
[2] *Science and Technology on Transient Physics Laboratory, Nanjing University of Science & Technology, Nanjing 210094, China;*
[3] *Faculty of Engineering, University of Nottingham, Nottingham NG72RD, UK*

Turbulent control and drag reduction in a channel flow via a bidirectional traveling wave induced by spanwise oscillating Lorentz force have been investigated in the paper. The results based on the direct numerical simulation (DNS) indicate that the bidirectional wavy Lorentz force with appropriate control parameters can result in a regular decline of near-wall streaks and vortex structures with respect to the flow direction, leading to the effective suppression of turbulence generation and significant reduction in skin-friction drag. In addition, experiments are carried out in a water tunnel via electro-magnetic (EM) actuators designed to produce the bidirectional traveling wave excitation as described in calculations. As a result, the actual substantial drag reduction is realized successfully in these experiments.

turbulence control, direct numerical simulation, channel flow, Lorentz force, drag reduction

1 Introduction

The surfaces of most aircrafts and transport vehicles are enwrapped by wall turbulence, whose coherent structures, characterized by streaks and longitudinal vortex, are responsible for the generation of high skin-friction drag. Therefore, reducing the intensity of wall turbulence can lead to drag reduction and speed increase [1–4]. Among available flow control techniques, the Lorentz force control has been studied extensively, which can induce a motion of electrically conducting fluids as a body force, and might then lead to turbulence suppression and drag reduction. Furthermore, it is possible to conduct many different types of Lorentz force by simply rearranging the electrodes and the magnets [5].

*Corresponding author (email: Kwing-So.Choi@nottingham.ac.uk)

Many numerical simulations studied by Berger et al. [6], Lee et al. [7], Du et al. [8], Satake et al. [9] and more recently experimental observations by Pang et al. [10] indicated that a remarkable turbulent drag reduction of more than 40% can be made with spanwise oscillating Lorentz forces described by

$$f_z = A e^{-y/\Delta} \sin\left(\frac{2\pi}{T} t\right), \tag{1}$$

where y and z are normal and spanwise coordinates, respectively, A is the amplitude of excitation of the EM actuator, Δ the effective penetration of the Lorentz force, T the period of the oscillation, and t the time. A recent investigation by the authors [11,12] both experimentally and numerically further confirmed the above results.

Du & Karniadakis [13] and Du et al. [8] reported that an efficient drag reduction can be achieved by using a

spanwise traveling Lorentz force, varied continuously both spatially and temporally, given by

$$f_z = A e^{-y/\Delta} \sin\left(\frac{2\pi}{\lambda_z} z - \frac{2\pi}{T} t\right), \tag{2}$$

where λ_z is the wave length in the span. This force transmits energy via a traveling wave along the spanwise direction. They found a formation of low-speed ribbons near the wall, and more than 30% reductions in skin-friction drag could be obtained. This work was experimentally followed by Xu and Choi [14], and similar control results were also obtained.

Huang et al. [5] explored a streamwise traveling force, i.e.,

$$f_z = A e^{-y/\Delta} \sin\left(\frac{2\pi}{\lambda_x} x - \frac{2\pi}{T} t\right), \tag{3}$$

where x is the streamwise coordinate, and λ_x is the wave length in the streamwise direction. Their DNS results showed this forcing was also capable of modifying near-wall flow and could lead to a large drag reduction of more than 40%.

An idealized force, referred to as "bidirectional wavy Lorentz force" with the form written as eq. (4), acts in the spanwise direction, and transmits energy along both the streamwise and spanwise directions in electrically conducting fluids,

$$f_z = A e^{-y/\Delta} \sin\left(\frac{2\pi}{\lambda_x} x + \frac{2\pi}{\lambda_z} z - \frac{2\pi}{T} t\right). \tag{4}$$

Apparently, the number of instantaneously triggered EM units to form the bidirectional wavy force is smaller than the spanwise oscillating Lorentz force, as well as the unidirectional traveling wavy Lorentz force, which means the consumed energy is less in the bidirectional wavy Lorentz force compared with the other methods. Therefore an efficiency improvement may be obtained by this method. However few works have been done into this control strategy up to now.

In this paper, the control of turbulent channel flow via bidirectional wave induced by a spanwise oscillating Lorentz force is investigated both numerically and experimentally. By the direct numerical simulation (DNS), the results suggest that the skin-friction drag can be reduced significantly by the imposed force with appropriate control parameters. Based on the calculated results, an EM actuator is designed. Subsequently, experiments are carried out in a water tunnel, where the substantial drag reduction is realized successfully.

2 Numerical scheme

The schematic of the turbulent channel flow adopted in this study is shown in Figure 1, where the computational domain is L_x by L_y by L_z, in the streamwise, normal, and spanwise directions, respectively. $U(y)$ is the mean flow in the x-direction. The Lorentz force is applied at the lower wall of the channel. Due to the exponential decay of the Lorentz force field, the turbulence structure over the upper wall is practically unaffected.

The incompressible Navier-Stokes equations with a body force term are

$$\frac{\partial \boldsymbol{u}}{\partial t} + \boldsymbol{u}\cdot\nabla\boldsymbol{u} = -\frac{1}{\rho}\nabla p + \nu\nabla^2\boldsymbol{u} + \frac{1}{\rho}(\boldsymbol{J}\times\boldsymbol{B}), \tag{5}$$

$$\nabla\cdot\boldsymbol{u} = 0, \tag{6}$$

$$\boldsymbol{J}\times\boldsymbol{B} = (0, 0, F_z), \tag{7}$$

here, $\boldsymbol{u}$ is velocity vector, t the time, ρ the fluid density, p the pressure, ν the kinematic viscosity, $\boldsymbol{J}$ the current density vector, $\boldsymbol{B}$ the magnetic flux density vector, and F_z the Lorentz force given by

$$F_z = St e^{-y/\Delta} \sin\left(\frac{2\pi}{\lambda_x} x + \frac{2\pi}{\lambda_z} z - \frac{2\pi}{T} t\right), \tag{8}$$

where, St is the amplitude of the Lorentz force at the lower wall of the channel.

In the simulations, the governing equations are placed in a nondimensional form by the centerline velocity U_c, the channel half-width h, current density and magnetic field values at the electrode and magnet surfaces, J_0 and B_0, respectively. Thus, the governing equations take the following nondimensional form:

$$\frac{\partial \boldsymbol{u}}{\partial t} + \boldsymbol{u}\cdot\nabla\boldsymbol{u} = -\nabla p + \nu\nabla^2\boldsymbol{u} + \boldsymbol{f}, \tag{9}$$

$$\nabla\cdot\boldsymbol{u} = 0, \tag{10}$$

$$\boldsymbol{f} = (0, 0, f_z), \tag{11}$$

$$f_z = A e^{-y/\Delta} \sin\left(\frac{2\pi}{\lambda_x} x + \frac{2\pi}{\lambda_z} z - \frac{2\pi}{T} t\right), \tag{12}$$

$$A = \frac{Sth}{\rho U_c^2} = \frac{J_0 B_0 h}{\rho U_c^2}. \tag{13}$$

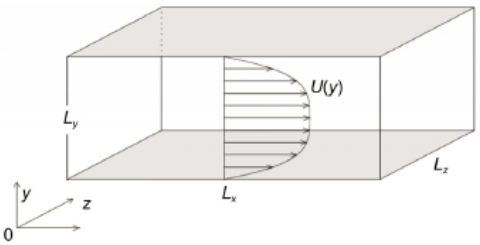

Figure 1 Schematic of turbulent channel flow.

Set $k_x = L_x/\lambda_x$ and $k_z = L_z/\lambda_z$ referred to as streamwise and spanwise wave numbers, respectively. Thus, the spanwise forcing f_z can be written further as:

$$f_z = A e^{-y/\Delta} \sin\left(\frac{2\pi}{L_x}k_x x + \frac{2\pi}{L_z}k_z z - \frac{2\pi}{T}t\right), \quad (k_x = L_x/\lambda_x,\ k_z = L_z/\lambda_z). \tag{14}$$

The numerical method adopted here to solve eqs. (9) and (10) is based on the standard Fourier-Chebyshev spectral method [15,16], which contains a dealiased Fourier method in the homogeneous directions i.e. streamwise and spanwise directions, and a Chebyshev-τ method in the wall normal direction. The boundary conditions are periodic in the homogeneous directions, and no-slip at the walls. Time integration of eq. (9) is made using a semi-implicit back-differentiation formula method with third-order accuracy. The linear term and the pressure term of the equation are evaluated by a Chebyshev-τ influence-matrix method. In addition, aliasing errors in the Fourier expansion for the nonlinear terms are removed by spectral truncation method referred to as 3/2-rule.

The bulk mean velocity averaged over the channel cross-section is fixed at U_m=2/3, and the corresponding bulk Reynolds number is Re_m=2666. Different combinations of computational domains and grid sizes were firstly tested in turbulent channel flow without control. Flow results indicate that a computational domain of $4\pi/3\times2\times2\pi/3$ (L_x^+=754 by L_y^+=360 by L_z^+=377) using a grid size of 64×65×32 is adequate for our purposes. Here, the superscript "+" indicates quantities in wall units, i.e. made non-dimensional by the friction velocity u_τ in unperturbed turbulent channel and the kinematic viscosity ν.

3 Results and discussions

As depicted by eq. (14), control results of bidirectional traveling wavy Lorentz force with fixed penetration length Δ, are effected by oscillation parameters (T and A) and wave numbers (k_x and k_z). Here we take cases with Δ=0.02, A=0.5 and T=10.0 (in which a better drag reduction can be obtained by spanwise oscillating Lorentz force, i.e., k_x=0 and k_z=0).

3.1 Drag reduction

Figure 2(a) describes the effects of the wave numbers k_x and k_z on the drag reduction, and Figure 2(b) is the corresponding shaded contours in the k_x-k_z plane. As illustrated in Figure 2, drag reduction of 35% can be achieved under the control of spanwise oscillating Lorentz force (i.e., k_x=0 and k_z=0). On the horizontal k_x-axis, maximum drag reduction of up to 45% can be obtained at (k_x=4, k_z=0). On the vertical k_z-axis, the smaller wave number (i.e., the larger wavelength) corresponds to greater amount of drag reduction as reported by Du et al. [8]. When (k_x=0, k_z=1), drag reduction of 20% can be achieved. Off the axes, corresponding to the bidirectional wavy Lorentz force, the drag can be reduced significantly in the white regions near k_x-axis.

3.2 Near-wall flow

The intrinsic coherent structures of wall turbulence can be modulated by a spanwise Lorentz force [17]. Figure 4 shows snapshot distributions of spanwise velocity and streaks (described by streamwise velocity fluctuation, u'), as well as the vortex structures (drawn by the imaginary part of complex eigenvalues of the velocity gradient tensor [18]) near the wall with and without control.

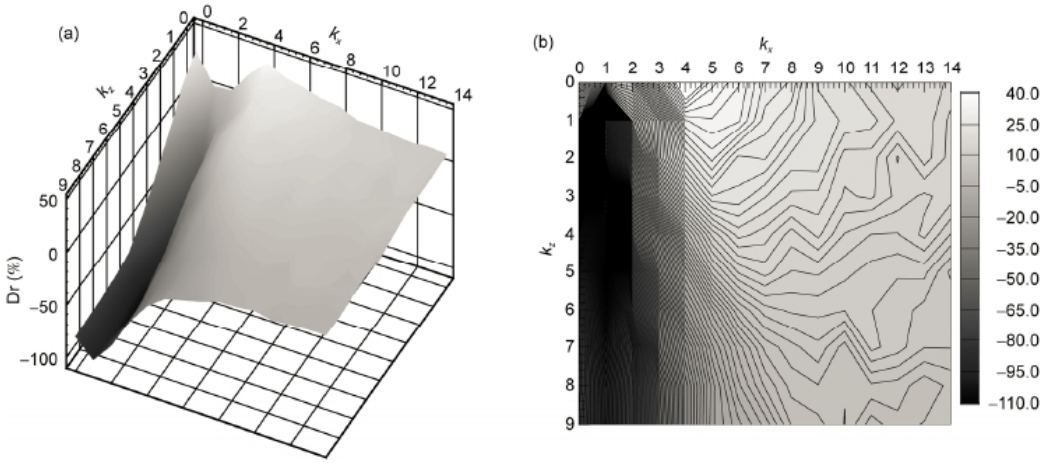

Figure 2 Drag reduction rate versus k_x and k_z with Δ=0.02, A=0.5, and T=10.

Figure 3(a) is for an uncontrolled flow, where a random and irregular instantaneous distribution of spanwise velocities is exhibited. The streaks do not always flow straight in the streamwise direction, but often meander in the spanwise direction. The longitudinal vortex structures are characterized by horseshoes vortices and quasi-streamwise vortices [5]. Figure 3(b) presents the flow subject to bidirectional wavy control with k_x=4 and k_z=1. White areas and black areas, representing, respectively, positive and negative values of spanwise velocities, incline to the right and alternate at x-z plane in the near-wall region. The streaks meander periodically, with similar appearance of the spanwise velocities. The horseshoes vortices disappear, and most of the remaining quasi-streamwise vortices are tilted to the positive spanwise direction. According to the theory proposed by Choi et al. [19], regular decline of near-wall streaks and vortex structures can lead to a generation of negative spanwise vorticity, resulting in the reduction of turbulent skin-friction drag. Also observed in Figure 3(b) are some longitudinal vortices elongated in the streamwise direction.

3.3 Turbulent bursting events

The near-wall regions of turbulent boundary layers are dominated by a sequence of bursting events associated with most of the turbulent production. The turbulent skin-friction drag is mainly contributed by the bursting events, which can be detected by the VISA (variable-interval space averaging) detective technique [20].

Figure 4 shows the conditionally sampled signatures of the burst signals detected by VISA and their corresponding shaded contours in the (x-z) plane at different y^+ position without and with bidirectional wavy forcing control. The effect of control on the bursting events is significant, especially at y^+=5.4, as shown in Figure 4(a). At this position, the burst space is reduced to less than half of that without control, and the intensity of the bursts (peak to peak value of the fluctuation at Δz^+=0) is reduced by 65%. Moreover, it should be noticed that the sampled signals of the controlled flow at y^+=5.4 has a significant sinusoidal feature in the spanwise direction, suggesting that bidirectional wavy control does modify the near-wall turbulent structures by introducing regular ejection and sweep motions close to the wall. At y^+=10 (see Figure 4(b)), where the effect of control on the burst signature is still strong, the burst space is about 1/3 of the uncontrolled case and the intensity of the burst is reduced by about 58%. At y^+=21, the effect of the forcing to the near-wall burst is minor, but we can still see about 25% reduction in the intensity. These remarkable changes in the burst signals in the near-wall region of the boundary layer imply a higher efficiency from the bidirectional wavy control.

3.4 Turbulence statistics

Figure 5(a) shows the effect of a bidirectional wavy control with k_x=4, k_z=1 on the mean velocity profile, compared with the uncontrolled profile. As commonly observed in turbulent control with drag reduction, the bidirectional wavy control shifts the mean velocity upward in the logarithmic region so that the viscous sublayer is thickened. The root mean square (r.m.s.) of the velocity components are shown in Figure 5(b). Both the streamwise and the normal velocity components for the controlled flow are reduced across the entire channel, suggesting turbulence production and the turbulent kinetic energy are suppressed. Figure 5(c), about the profiles of the r.m.s. of the vorticity components, is clearly indicates the streamwise vorticity component increases near the wall as control. These trends are very similar to those reported by Pang et al. [10] and Du et al. [8] in the spanwise oscillating Lorentz force and the spanwise traveling wavy Lorentz force respectively. Kim et al. [3]

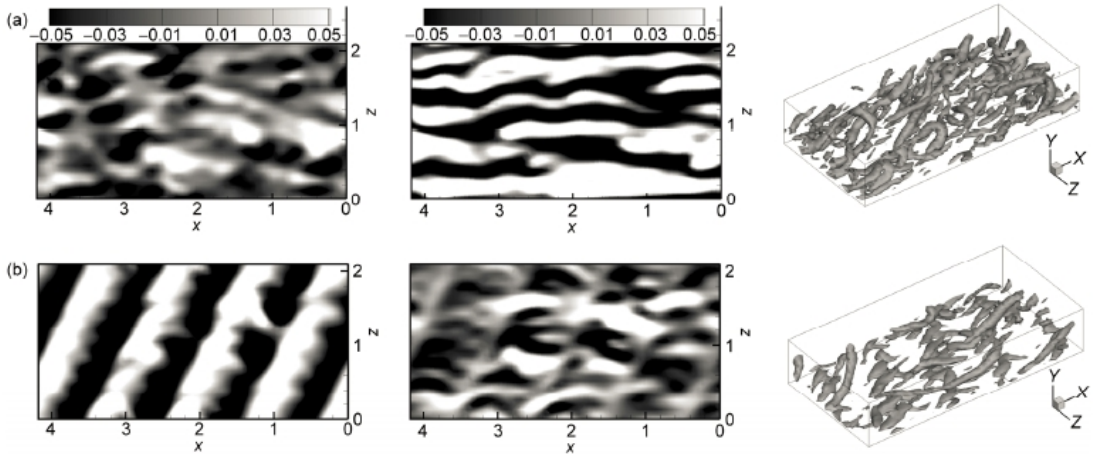

Figure 3 The instantaneous distributions of spanwise velocity (left), streaks (middle) and vortex structures (right) in the near-wall region. (a) No control; (b) k_x=4, k_z=1.

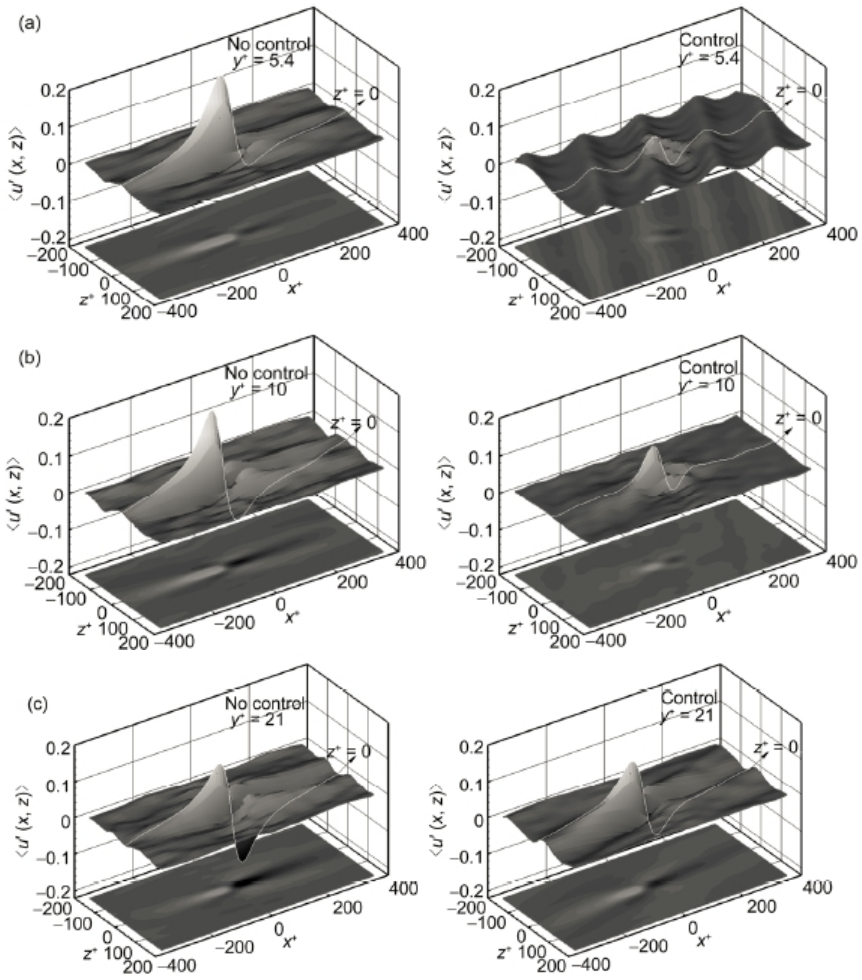

Figure 4 Conditional averages of fluctuating streamwise velocities with a contour map in the x-z plane at different y^+ positions. The first column without control, and the second column with k_x=4 and k_z=1 control.

have identified the peak of r.m.s. streamwise vorticity in uncontrolled flow located at $y^+ \approx 20$ as the centre of the streamwise vortices. This peak disappears in the controlled flow, indicating an elimination of streamwise vortices [21].

4 Experimental validation

For validation, a water tunnel test was conducted using specially designed EM actuators. A key element in the experiment is producing the required bidirectional traveling wave excitation.

4.1 EM actuators

A unit of the EM actuator used is illustrated in Figure 6. Permanent magnets and electrodes are lined up in the streamwise direction alternately, where N and S denote the north and south polarity of the magnets, respectively. The electrodes are activated alternatively so that the required bidirectional traveling wave excitations can be produced. The electrodes are activated following a pre-set phase change via a PLV controller. For example, the black color indicates positively activated electrode, dark gray denotes negatively activated electrode, and light gray not-activated. Figures 7(a)–(d) illustrate 4 phases of an EM unit. The polarity of the electrodes alternates periodically. Solid arrows denote the local forcing direction. Flow is from right to left. Hollow arrows denote the expected traces of the local flow.

Figure 8 shows the material object photograph of the EM actuator, which consists of a stainless steel plate equipped with magnets (see Figure 8(a)) and a copper electrode sheet (see Figure 8(b)). The whole EM actuator consists of 8 electro-magnetic units, covering a streamwise distance of 420 mm and a spanwise distance of 420 mm. The dimensions are selected so that it can control around 10 low-speed streaks whose length in the streamwise direction is around 1000 wall units and spanwise spacing is about 100 wall units. Each permanent magnet is made of 5 mm wide. The

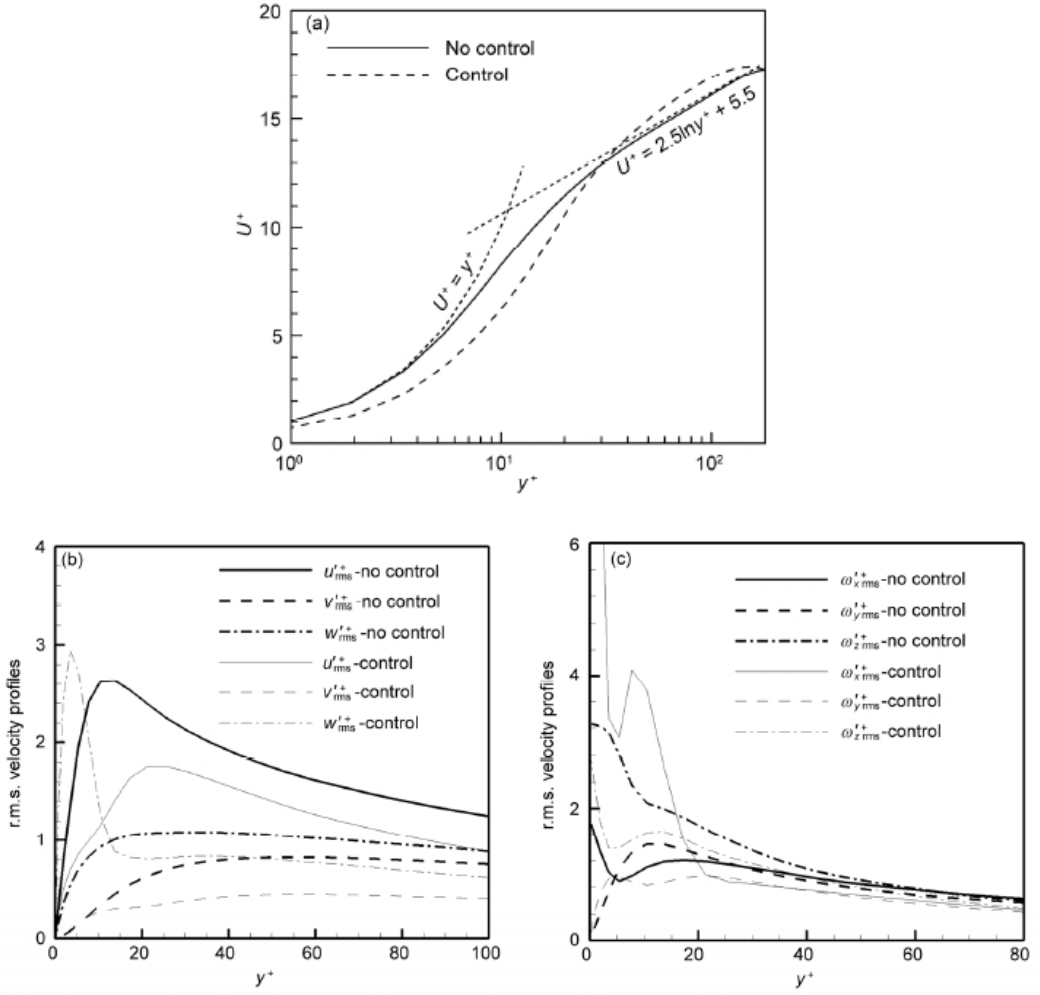

Figure 5 Profiles of (a) mean streamwise velocity, (b) velocity and (c) vorticity turbulence intensities.

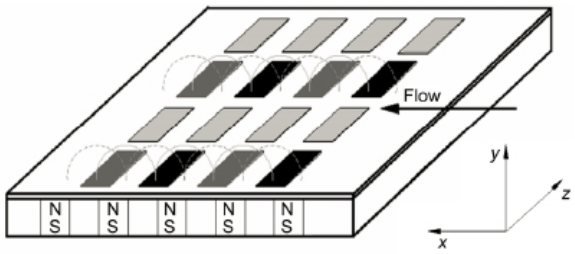

Figure 6 Configuration of an electro-magnetic unit. The black color indicates positively activated electrode, dark gray denotes negatively activated electrode, and light gray not-activated.

magnetic field strength at wall is 1.2 T. The electrode is 12 mm long by 5 mm wide by 0.017 mm thick. When the polarity of the electrodes alternates periodically as described in Figure 7, the Lorentz force is induced, which acts in the spanwise direction, and transmits energy along the streamwise direction and spanwise direction at the same time in electrically conducting fluids with wave numbers k_x=4 and k_z=2.

4.2 Experimental system

The experiment was conducted in a plexiglass water tunnel with an observation section of 1300 mm×300 mm×290 mm, as shown in Figure 9. The center line velocity of the observation section was set at 0.057 m/s, and the corresponding centerline Reynolds number is Re=8500. The working medium was salt water with a concentration of 3%. The test plate equipped with two electro-magnetic actuators was placed in the replaceable test surface of a float bed, which was hung in the observation section of water tunnel, and kept flush to the wall surface. In the experiment, the float bed had a displacement along the flow direction due to the wall shear stress, which can be measured by a displacement transducer. The driving voltage provided by the PLV controller was fixed at 30 V, with the oscillating frequency set at 0.5 Hz. By switching the polarity of electric current, the direction of the created spanwise Lorentz force can be altered periodically, and the required traveling wave excitation can be produced. The evolution of the flow in the near-wall region was recorded through a PIV system. For more details refer to the author's previous work [22].

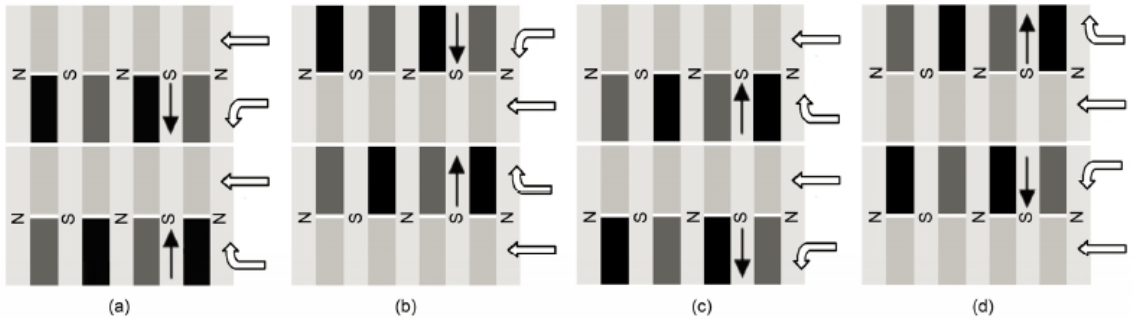

Figure 7 Electrodes energized with alternating polarity in a control period of the actuations.

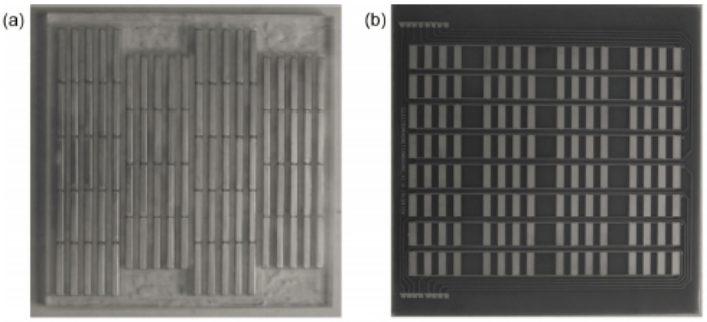

Figure 8 Photograph of the EM actuator. (a) Stainless steel plate equipped with magnets; (b) electrode sheet.

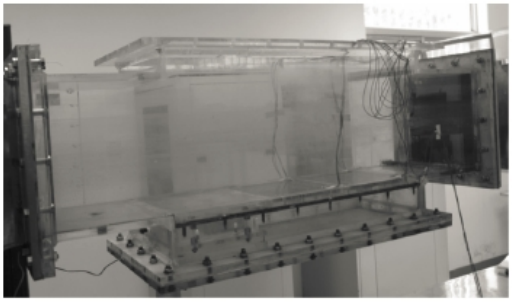

Figure 9 Observation section of the water tunnel.

4.3 Experimental results

Figure 10 shows a series of flow visualization pictures, illustrating the time evolution of flow field in a control period, where Figures 10(a)–(d) correspond to 4 phases of the EM units respectively (see Figure 7). Flow is from right to left. It is clearly seen that the traces of local flow appear as expected in Figure 7. Figure 10(a) shows that the intake flow masses to the second row of the EM units. In the second phase as seen in Figure 10(b), the intake flow masses to the third row following the traveling-wave moving direction. In the third phase, the mass region formed in the second phase is propagated further to the top row. At the final fourth phase, the new mass region is formed at the first row and then a cycle is completed. Also observed from Figure 10 is that the trace of the flow is significantly sinusoidal in the streamwise direction. These characteristics reflect the bidirectional traveling wavy Lorentz force.

The change of the mean wall shear stress can be obtained by the drag measurement system. The statistical results indicate that a reduction of approximately 10% on the mean wall shear stress can be achieved. The experiments have lower performance than the DNS, because the actual Lorentz force produced by the EM actuators cannot approach that of the idealized simulation. Moreover, neither edge effects nor the development distance are present in the DNS owing to periodic boundary conditions.

5 Conclusion

Direct numerical simulations are performed to investigate the control effects of the bidirectional traveling wavy Lorentz force on a turbulent channel flow. The results show that the drag reduction strongly depends on the control parameters, and appropriate combinations of control parameters can result in the regular decline of near-wall streaks and vortex structures with respect to the flow direction, leading to effective suppression of turbulence production and significant reduction in skin-friction drag. Based on the simulations, an electro-magnetic actuation system is designed, and associated experimental research is carried out in a water tunnel. Experimental results indicate that actual drag reduction can be achieved via the bidirectional traveling

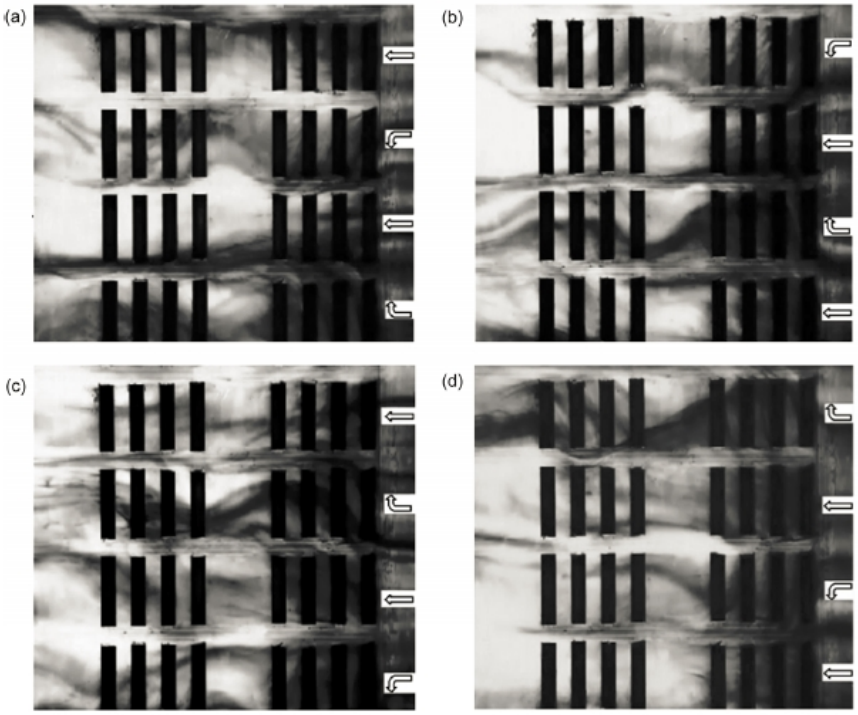

Figure 10 Flow visualization with the bidirectional traveling Lorentz force (top view). Flow is from right to left. Hollow arrows on the right side of the pictures denote the expected traces of local flow direction.

wave with optimal control parameters produced by the electro-magnetic actuators.

This work was supported by the National Natural Science Foundation of China (Grant Nos. 11172140 and 11202102), the Specialized Research Fund for Doctoral Program of Higher Education (Grant No. 20123219120050), and the EU FP6 Framework Program AVERT and the Faculty of Engineering, University of Nottingham.

1 Xu C X, Deng B Q, Huang W X, et al. Coherent structures in wall turbulence and mechanism for drag reduction control. Sci China-Phys Mech Astron, 2013, 56(6): 1053–1061
2 Sun Z S, Ren Y X, Laricq C. Drag reduction of compressible wall turbulence with active dimples. Sci China-Phys Mech Astron, 2011, 54(2): 329–337
3 Kim J, Moin P, Moser R. Turbulence statistics in fully developed channel flow at low Reynolds number. J Fluid Mech, 1987, 177: 133–166
4 Ge M W, Xu C X, Cui G X. Transient response of Reynolds stress transport to opposition control in turbulent channel flow. Sci China-Phys Mech Astron, 2011, 54(2): 320–328
5 Huang L P, Fan B C, Dong G. Turbulent drag reduction via a transverse wave traveling along streamwise direction induced by Lorentz force. Phys Fluids, 2010, 22(1): 015103
6 Berger T W, Kim J, Lee C, et al. Turbulent boundary layer control utilizing the Lorentz force. Phys Fluids, 2000, 12(3): 631–649
7 Lee C, Kim J. Control of the viscous sublayer for drag reduction. Phys Fluids, 2002, 14(7): 2523–2529
8 Du Y Q, Symeonidis V, Karniadakis G E. Drag reduction in wall-bounded turbulence via a transverse travelling wave. J Fluid Mech, 2002, 457: 1–34
9 Satake S, Kasagi N. Turbulence control with wall-adjacent thin layer damping spanwise velocity fluctuations. Int J Heat Fluid Flow, 1996, 17(3): 343–352
10 Pang J, Choi K S. Turbulent drag reduction by Lorentz force oscillation. Phys Fluids, 2004, 16(5): 35–38
11 Mei D J, Fan B C, Huang L P, et al. Drag reduction in turbulent channel flow utilizing spanwise oscillating Lorentz force (in Chinese). Atca Phys Sin, 2010, 59(10): 6786–6792
12 Mei D J, Fan B C, Chen Y H, et al. Experimental investigation in turbulent channel flow utilizing spanwise oscillating Lorentz force (in Chinese). Atca Phys Sin, 2010, 59(12): 8335–8342
13 Du Y Q, Karniadakis G E. Suppressing wall-turbulence by means of a transverse traveling wave. Science, 2000, 288: 1230–1234
14 Xu P, Choi K S. Boundary layer control for drag reduction by Lorentz forcing. In: Proceedings of Flow Control and MEMS. Berlin: Springer, 2007. 259–265
15 Canuto C, Hussaini M Y, Quarteroni A, et al. Spectral Methods in Fluid Dynamics. New York: Springer-Verlag, 1988. 201–212
16 Huang W X, Xu C X, Cui G X, et al. Mechanism of drag reduction by spanwise wall oscillation in turbulent channel flow (in Chinese). Chin J Theor Appl Mech, 2004, 36(1): 24–30
17 Huang L P, Fan B C, Dong G. Turbulent drag reduction via a streamwise traveling wave induced by spanwise wall oscillation (in Chinese). Chin J Theor Appl Mech, 2011, 43(2): 277–281
18 Zhou J, Adrian R J, Balachandar S, et al. Mechanisms for generating coherent packets of hairpin vortices in channel flow. J Fluid Mech, 1999, 387: 353–396
19 Choi K S, Clayton B R. The Mechanism of turbulent drag reduction with wall oscillation. Int J Heat Fluid Flow, 2001, 22: 1–9
20 Kim J. Turbulence structures associated with the bursting event. Phys Fluids, 1985, 28(1): 52–58
21 Zhao H, Wu J Z, Luo J S. Turbulent drag reduction by traveling wave of flexible wall. Fluid Dyn Res, 2004, 34: 175–198
22 Huang L P, Fan B C, Mei D J. Mechanism of drag reduction by spanwise oscillating Lorentz force in turbulent channel flow. Theor Appl Mech Lett, 2012, 2(1): 012005